Materials Science in Semiconductor Processing 152 (2022) 107050

Contents lists available at ScienceDirect

Materials Science in Semiconductor Processing

journal homepage: www.elsevier.com/locate/mssp

# Density functional theory studies of the structural, optoelectronic, bond stiffness and lattice dynamical properties of double perovskite oxides $M_2YVO_6$ (M= Mg, Sr): Promising candidates for optoelectronic applications

Muhammad Iqbal Hussain [a,b,*], R.M. Arif Khalil [a,**]

[a] Materials Simulation Research Laboratory (MSRL), Department of Physics, Bahauddin Zakariya University Multan, 60800, Pakistan
[b] Department of Physics, University of Education, Lahore, Multan Campus, 54000, Pakistan

ARTICLE INFO

*Keywords:*
Optical properties
Optoelectronics
Dynamical stability
Photonic energy

ABSTRACT

The double perovskite type oxides are deemed to be an eloquent materials to be used for applications in efficient optoelectronic devices/transducers. In order to explore physical properties of $M_2YVO_6$; (M = Mg, Sr) perovskites Full potential Linearly Augmented Plane Wave (FPLAPW) method is used in the frame work of WIEN2K code. LDA + U functional has been preferred here for getting an accurate and systematic results associated to the electronic and optical response of these compounds. These compounds fall into semiconductor category showing direct energy band gap of 1.45 eV ($Mg_2YVO_6$) and 0.82 eV ($Sr_2YVO_6$). Appearance of the energy states of different level in the conduction regions of both compounds fortify the view point that the valence electrons may jump to these states while enhancing conductivity of such devices (i.e., solar cells) whichever are fabricated for producing eternal energy. Projected density of states (PDOS) confirm the presence of $Mg^{2+}/Sr^{2+}$, $Y^{3+}$, $V^{5+}$, $O^{2-}$ in the $M_2YVO_6$ where M = Mg, Sr. In addition to it, optical analysis shows that these materials reflect very little electromagnetic radiations when fall on their surfaces. $Sr_2YVO_6$ holds relative bond stiffness greater than its standard value of ½ while it is less than half for $Mg_2YVO_6$. Phonons analysis shows few soft modes of frequency in case of $Mg_2YVO_6$ which might be due to particular orientation of monoclinic phase of the crystal structure, whereas no imaginary modes of vibrations are observed for $Sr_2YVO_6$. It looks very fabulous to claim that these compounds might be an appealing ones for optoelectronic applications due to their huge absorption rate/optical conduction ability, which also declares them very suitable materials for devising transducers.

## 1. Introduction

Within the long history of materials, double perovskite (DP) oxides had been appealing to the researchers from the long past. They have stoichiometric formula as $A_2B'B''O_6$ wherein A-cited large cations may be divalent or trivalent metals and B-cited ($B', B''$) small cations can be heterovalent transition metals. The crystal structure and space group of double perovskites mainly depend on the arrangement of $B'O_6$ and $B''O_6$ octahedra, especially their ordering and tilting [1–3]. Some physical properties like structural, electronic and thermodynamic behavior of tungstate based double perovskite oxides $Ba_2XWO_6$ (X = Mg, Ni, Zn) were explored in 2013 where these compounds have been found to be semiconducting materials [4]. However, their band gap values were reported 10% less as compared to the formerly reported experimental values, the inconsistency in their values to the extent of 10% might has been occurred due to the implementation of an inappropriate density functional/simulation code. Literature reveals that experimental efforts were also vested on a series of lead free double perovskites ($Ln_2NiMnO_6$; Ln = La, Eu, Dy, Lu) to shed some light on their applications in photovoltaics [5]. One compound amongst our considered series, $Mg_2YVO_6$ was characterized experimentally very first time in 2015 by Su et al. [6] to the extent that they have deliberated its microwave dielectric behavior only in tetragonal phase through X-Ray Diffraction Analysis. Later, in 2019 Alsabah et al. [7] who got inspired from the work of Su et al., have extended discussion about two perovskites, i.e., $A_2YVO_6$ (A = Mg, Sr) and synthesized their structural and optical properties for the first time while using solid state reaction methods.

As per literature about DP, renowned international journal (Energy

* Corresponding author. Materials Simulation Research Laboratory (MSRL), Department of Physics, Bahauddin Zakariya University Multan, 60800, Pakistan.
** Corresponding author.
*E-mail addresses:* miqbal@ue.edu.pk (M.I. Hussain), muhammadarif@bzu.edu.pk (R.M.A. Khalil).

https://doi.org/10.1016/j.mssp.2022.107050
Received 22 February 2022; Received in revised form 4 August 2022; Accepted 11 August 2022

& Environmental Science) of Royal Society of Chemistry in 2019 had attributed the work of Yin et al. [8] and recognized high efficiency of converting light into electrical energy through diverse range of processes such as photocatalysis, photovoltaics etc. which could merely been established if double perovskites are used to devise such devices. In very recent past 2020, Kangsabanik and co-workers [9] has also established a theoretical view point in their study on $Na_2XIO_6$ (X = Bi, In) that double perovskite oxides may be chosen as promising materials for devising photovoltaics and photo-electrochemical cells. Moreover, three years earlier from now, it was interpreted that double perovskite oxides, where A-site cations are small in size, not only exhibit unusual characteristics at ambient pressure and temperature, but also unveil their veracity of being utilized in diverse domain of optoelectronic applications [10]. History of DPs is not only full of glamorous results in miscellaneous fields of physics but in materials chemistry as well. So none of us can refute their importance. The values of energy band gap calculated for our combinations of double perovskites are approximately close to the magnitude of the gaps formerly reported for different combinations $Ba_2ErTaO_6$ (2.50 eV) and $Ba_2TmTaO_6$ (2.40 eV) [11], which in fact endorse consistency in our results. Another study about DP oxides have clued that these are best semiconductors which have been potential materials for diverse range of applications, particularly, these are deemed fit for wasted energy regeneration due to their significant figure of merit [12]. Also the study on periodates such as $Na_2BIO_6$ (B═Bi, In) in monoclinic phase vested by J. Kangsabanik and his co-worker [13] strongly corroborates the researcher's general perception and strengthen our narrative that DPs may be an alternative materials to substitute the prevalent ones being used for devising optoelectronic devices. Apart from the studied characteristics, previously various combinations of DPs have not only been deliberated to the extent of some selected physical properties, but also their magnetism is found to be discussed numerously [14,15].

In the literature heretofore no researcher had made his exclusive efforts towards exploration of the considered combinations ($M_2YVO_6$; M = Mg, Sr) while using WIEN2K, a versatile simulator. Nonetheless, experimental efforts were put into some extent for questing their structural and dielectric properties only. Which however seem insufficient for any material to be explored prior to its commercialization. Also, endorsement of the results (whether based on experiments or theories) of any material through a series of different approaches has always been a mystified challenge to the researchers; which is ought to be endorsed for the considered compounds as well. This plausible challenge has motivated us to systematically discuss these two combinations ($M_2YVO_6$; M = Mg, Sr) from the perovskites' family to determine their structural, optoelectronic, bond stiffness and phonon frequencies by using FPLAPW in the framework of WIEN2K.

## 2. Computational approach

The physical properties of $M_2YVO_6$; M = Mg, Sr (DP) are envisioned by using DFT based WIEN2K simulator with auxiliary assistance of FPLAPW method for consistency and accuracy [16]. The wave function within the sphere was taken up to $l_{max} = 10.0$. In order to determine size of matrices (size of basis sets), the value of $R_{mt}K_{max}$ was set as 7. As per provision in the WIEN2K code, lattice parameters were got optimized while reducing muffin radius by 7.5% by using PBE-GGA along with Hubbard (LDA + U) functional. The exchange integral J was set to zero, whereas the Hubbard 'U' values was set to $U_{eff}$ = U-J such as 2.0 eV and 2.5 eV for '*d*' orbitals of yttrium and vanadium elements, respectively. Here we took 1000 sampling k-points in the 1st Brillouin Zone (BZ) of the studied compounds for extracting numerical data to predict their physical behavior. Cutoff energy was fixed as −9.0 eV. Gaussian smearing value was fixed to 0.1 eV in order to reduce noise/variations and seeking legible peaks/electronic behavior [17,18]. Convergence energy equal to 1.36 eV was set to achieve stability and convergence of the considered many body systems. Kramers–Kronig [19,20] relations which inter-link the real and imaginary components of any complex function were computationally assisted to envision an optical response of $M_2YVO_6$; M = Mg, Sr. Density-functional-perturbation-theory (DFPT) [21] approach has been used in order to hunt for dynamical stability.

**Table 1**
The unit cell dimensions of optimized monoclinic crystal structure of $M_2YVO_6$; (M = Mg, Sr) with $P2_1/n$ space-group symmetry.

| Elements | x | y | z |
|---|---|---|---|
| $Mg^{2+}/Sr^{2+}$ | 0.50000 | 0.97660 | 0.25000 |
| | 0.50000 | 0.02340 | 0.75000 |
| | 0.00000 | 0.47660 | 0.25000 |
| | 0.00000 | 0.52340 | 0.75000 |
| $Y^{3+}$ | 0.00000 | 0.00000 | 0.00000 |
| | 0.50000 | 0.50000 | 0.50000 |
| $V^{5+}$ | 0.00000 | 0.00000 | 0.50000 |
| | 0.50000 | 0.50000 | 0.00000 |
| $O^{2-}$ | 0.28800 | 0.77620 | 0.96812 |
| | 0.71110 | 0.22380 | 0.03188 |
| | 0.21110 | 0.27620 | 0.53188 |
| | 0.78890 | 0.72380 | 0.46812 |
| | 0.22380 | 0.28890 | 0.96812 |
| | 0.77620 | 0.71110 | 0.03188 |
| | 0.27620 | 0.78890 | 0.53188 |
| | 0.72380 | 0.21110 | 0.46812 |
| | 0.06380 | 0.01210 | 0.25640 |
| | 0.93620 | 0.98790 | 0.74360 |
| | 0.43620 | 0.51210 | 0.24360 |
| | 0.56380 | 0.48790 | 0.75640 |

**Table 2**
It presents value of the optimized lattice constant $a_o$(Å), bulk modulus $B_o$(GPa), derivative of the bulk modulus with respect to pressure ($B_o^{'}$), the ground state energy $E_o$(Ry) and volume ($V_o$) at equilibrium state at zero pressure by using LDA + U.

| Parameters | Mg2YVO6 | Sr2YVO6 |
|---|---|---|
| $a_o$ (Å) | a = 5.3226 | a = 6.2576 |
| | b = 5.3290 | b = 6.2651 |
| | c = 7.5277 | c = 8.8501 |
| Cell angles | $\alpha = \gamma = 90^0$ | $\alpha = \gamma = 90^0$ |
| | $\beta = 90.022^0$ | $\beta = 90.022^0$ |
| $B_o$(GPa) | 154.45 | 139.53 |
| $B_o^{'}$ | 4.91 | 4.33 |
| $E_g$(eV) | 1.45 | 0.82 |
| $E_o$(Ry) | −20750.50 | −44587.50 |
| $V_o$ (a.u.$^3$) | 1672.29 | 1831.27 |

## 3. Results and discussion

### 3.1. Structural properties

Here the monoclinic phase of the crystal structures of $M_2YVO_6$; M = Mg, Sr (double perovskites) has been discussed within their symmetry phase of $P2_1/n$. Wyckoff positions of their constituent atoms, i.e., $Mg^{2+}/Sr^{2+}$, $Y^{3+}$, $V^{5+}$ and $O^{2-}$ are 4e, 2a, 2b and 4e respectively. The unit cell dimensions of optimized monoclinic crystal structures are summarized in Table 1. The cell parameters (Å) are summarized in Table 2. The single-point calculations approach is entrusted for both unit cells in order to get their optimized lattice constants at the ground state. While ignoring effects of polarization and other interactions in the systems, it is noticed that the cell parameters/sizes increase from Mg to Sr in line with the size of cations $Mg^{2+}$(0.86 Å) < $Sr^{2+}$(1.32 Å). The cell size and ionic radii of the said cations are found to be associated excellently. The optimized unit cell dimensions for $Mg_2YVO_6$ are found to be 'a = 5.3226 Å, b = 5.3290 Å, c = 7.5277 Å' and while for $Sr_2YVO_6$ these are noted as 'a = 6.2576 Å, b = 6.2651 Å, c = 8.8501 Å' where $\alpha = \gamma = 90^0$ & $\beta = 90.022^0$. The β angle is found very close to the right angle ($90^0$).

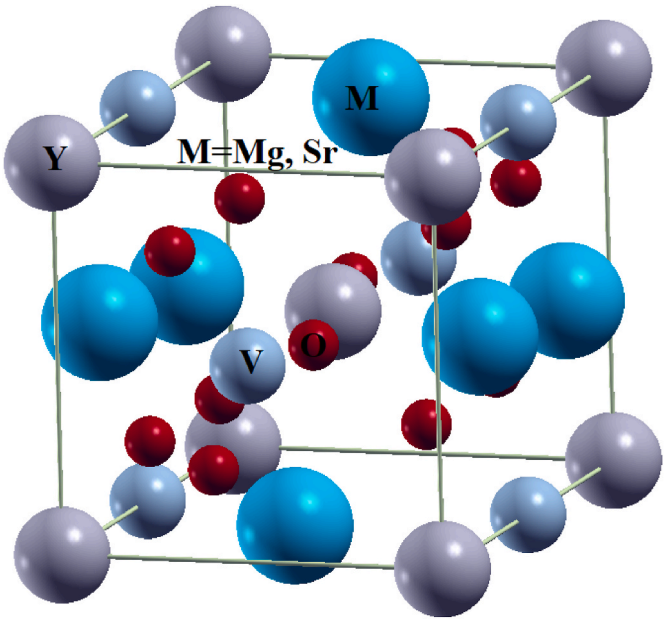


**Fig. 1.** Optimized crystal structure of $M_2YVO_6$; (M = Mg, Sr), where Turquoise, Grey, Light Gray and red spheres represent $Mg^{2+}/Sr^{2+}$, $Y^{3+}$, $V^{5+}$ and $O^{2-}$ ions respectively.

However, previous literatures [22] endorse deviation up to $0.05^0$ in monoclinic β angle of $90^0$. The minor deviation in β (*i.e.*$0.022^0$ in our cases) might has been noticed owing to large ionic radius of A-cations which may further be attributed to the slight distortions of the octahedral. In the present report, the lattice parameters follow an increasing trend *i.e.* c > a > b which can also be visualized from the optimized crystal structure, displayed in Fig. 1. Also we have determined ground state quantities, i.e., bulk modulus in order to observe resistance/hardness of the studied compounds under pressure, derivative of the bulk modulus which is customary a dimensionless quantity [23]. The negative sign with the ground state energies $E_o$(Ry) for both compounds signifies and ensures their structural stability and their magnitude reveals that these are chemically reasonable compounds. Moreover, bigger value of $E_o$(Ry) for $Mg_2YVO_6$ (−20750.50 Ry) shows that it would require large amount of energy to break the bonds between its constituents than it required (−44587.50 Ry) for its counterpart $Sr_2YVO_6$. Thus $Mg_2YVO_6$ can be declared harder than its counterpart, which can also be confirmed from greater value of its bulk modulus (154.45 GPa). So far as the volume $V_o$ (a.u.$^3$) calculated for both these compounds at equilibrium state shows similar increasing trend as par the size of their constituent A-cations $Mg^{2+}$(0.86 Å) < $Sr^{2+}$(1.32 Å). The tolerance factor ($\tau$) is indicator to seek suitability of combinations of cations in perovskites. It was calculated for $Mg_2YVO_6$ and $Sr_2YVO_6$ by the standard formula as reported by Alsabah et al. [7], Leng et al. [24] and Borchani et al. [25] in their recent work. For our compounds the magnitude of $\tau \sim 0.7$ fulfils the stability condition of the crystal structure with the phase symmetry of monoclinic ($P2_1/n$) (see Fig. 2).

$$\tau = -\frac{r_A + r_O}{\sqrt{2}\left(\frac{r_{B'}}{2} + \frac{r_{B''}}{2} + r_O\right)} \quad (1)$$

wherein $r_A$ presents the ionic radii of A-cited large cations, $r_{B'}/r_{B''}$ denotes the ionic radii of B-cited ($B'/B''$) small cations with $r_O$ the ionic radii of oxygen anion. Moreover, the cohesive energy per atom is a measure of the force strength that binds atoms together in the solid state. Also it can signify the structural stability of any material. It can be calculated with the following relation [11,12]:

$$E_{coh} = -\left[\frac{E^{tot}_{M_2YVO_6} - \left(a\ E^{tot}_M + b\ E^{tot}_Y + c\ E^{tot}_V + d\ E^{tot}_O\right)}{a + b + c + d}\right]_{isolated} \quad (2)$$

here $E^{tot}_{M_2YVO_6}$ is the total energy of the optimized crystal structures where M = (Mg, Sr), $E^{tot}_M$, $E^{tot}_Y$, $E^{tot}_V$ and $E^{tot}_O$ describe the total energy calculated for isolated constituent atoms in the compounds. The constant parameters a, b, c, d denominate the number of atoms in M = (Mg, Sr), Y, V and O elements, respectively. It is worth to state that cohesive energy is calculated after ensuring the structural optimization of these structures. Our results obtained for cohesive energy are noted to be 5.90 eV/atom for $Mg_2YVO_6$ and 6.20 eV/atom for $Sr_2YVO_6$. Positive values of $E_{coh}$ for both perovskites corroborate strong atomic bonding between their constituents. Whereas, the higher value of $E_{coh}$ measured for the later compound unveils that it is structurally more stable material to be preferred for optoelectronic applications.

### 3.2. Vibrational properties

The phonon analysis express not only vibratory behavior of the atoms but also interpret thermal conductivity and stability of the solid materials. Herein, DFPT approach is used in order to hunt for dynamical stability [21]. Then phonon modes (Raman and Infrared (IR) active) of vibration for $M_2YVO_6$; (M = Mg, Sr) perovskites are also determined. The plots of phonon dispersion curve with G-Z-Y symmetry points of the BZ and phonon density of states for $M_2YVO_6$; (M = Mg, Sr) are shown side by side in Figs. (3 and 4). Unfortunately for $Mg_2YVO_6$ few imaginary/soft modes of frequency are found up to −185.09 cm$^{-1}$ (as shown in Fig. 3(a)), which might be associated with its instable outlook to the extent of dynamics in particular orientation of monoclinic phase of the crystal structure. Such type of wacky behavior of perovskite oxides can generally be found in various former reports [26,27]. Nevertheless, $Sr_2YVO_6$ is found free from imaginary frequencies ensuring its dynamical stability as claimed by Baskurt and co-workers [28] in their former study about $VI_3$ (see Fig. 4).

The vibrational analysis/some important IR active and Raman active modes of vibrations for $M_2YVO_6$; (M = Mg, Sr) are summarized in

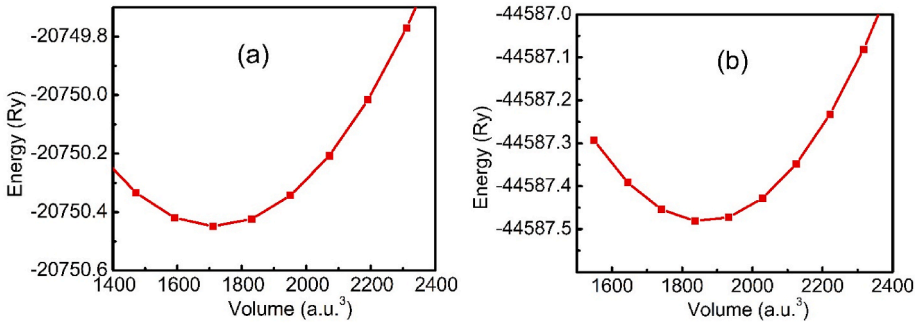


**Fig. 2.** Energy versus volume optimization graphs for (a) $Mg_2YVO_6$ and (b) $Sr_2YVO_6$.

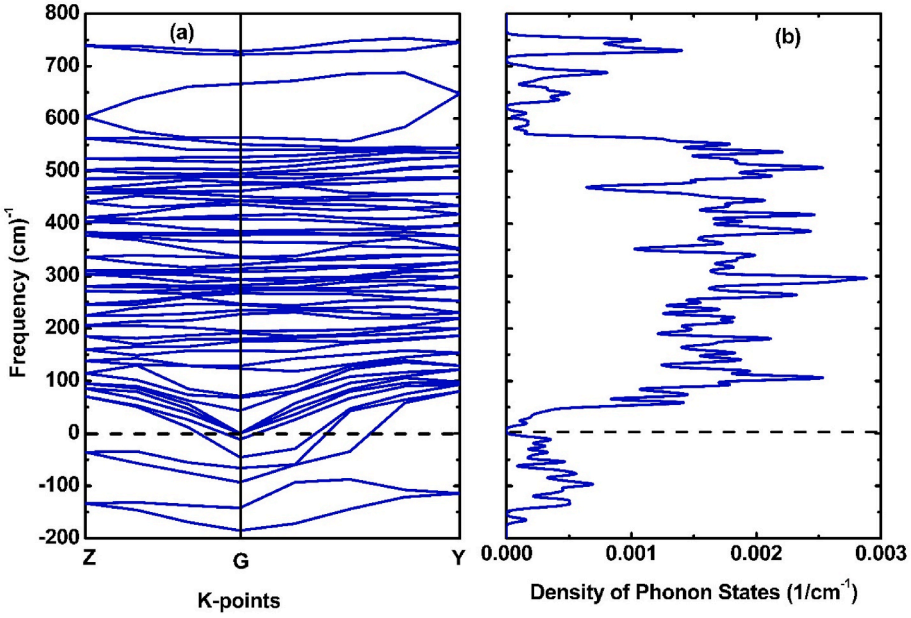


**Fig. 3.** The plots of phonon dispersion curves and density of phonon states vs frequency for $Mg_2YVO_6$ perovskite.

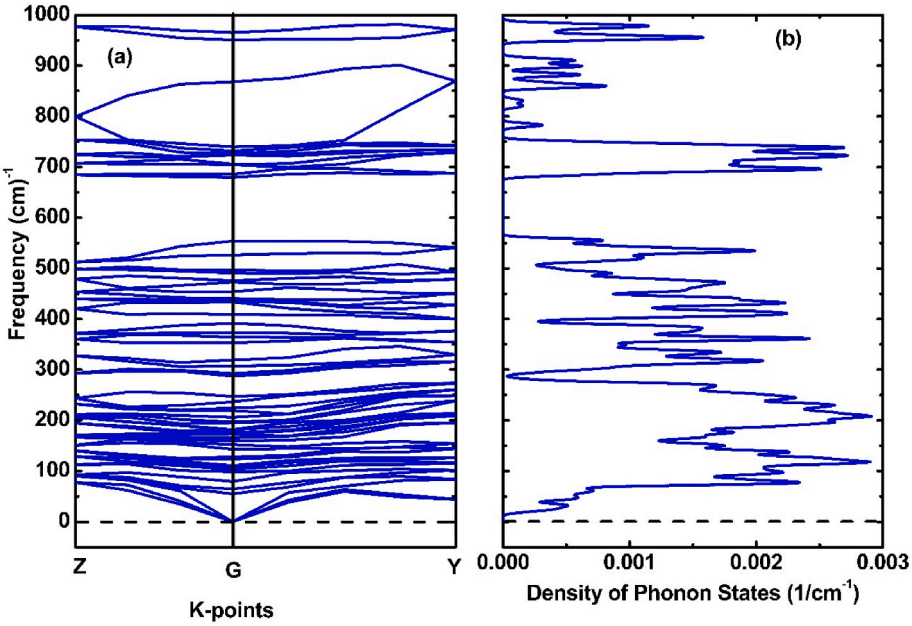


**Fig. 4.** The plots of phonon dispersion curves and density of phonon states vs frequency for $Sr_2YVO_6$ perovskite.

Table 3. In our both cases $Mg_2YVO_6$ and $Sr_2YVO_6$, out of 60 modes of vibrations (3 N), each compound contains three acoustic phonon modes of vibrations at zero frequency near G symmetry point. Here N represents number of atoms in unit cell structure. In case of $Mg_2YVO_6$ remaining 57 modes (associated to the optical modes of vibrations) are found to be split into 33 IR active modes and 24 Raman active modes of vibrations. So far as 57 optical modes of vibrations for $Sr_2YVO_6$, 33 are IR active while merely 05 modes are Raman active, remaining 19 modes of vibrations are inactive. As presented in Table 3, the lowest optical modes are found to be IR active at 43.41 $cm^{-1}$ and 55.33 $cm^{-1}$ frequencies, while the highest optical Raman active modes of vibrations are noticed at 728.28 $cm^{-1}$ and 965.29 $cm^{-1}$ frequencies for $Mg_2YVO_6$ and $Sr_2YVO_6$, respectively. Concentrated phonon density of states has been observed in the frequency range from 101.50 $cm^{-1}$ to 540.770 $cm^{-1}$ for $Mg_2YVO_6$, while these states are found to be maximum from 75.31 $cm^{-1}$ to 536.25 $cm^{-1}$ for $Sr_2YVO_6$ perovskite.

### 3.3. Electronic properties

The band structure plots for the studied compounds are shown in Fig. 5 (a & b). It is noted from band structure of $Mg_2YVO_6$ that valence band maxima (VBM) and conduction band minima (CBM) are coincident at the gamma (Γ) symmetry point of the BZ, resulting direct energy gap having value ~ 1.45 eV energy. Similarly for $Sr_2YVO_6$, VBM and CBM are happened at Γ symmetry point of the BZ with different value of the band gap, i.e., ~0.82 eV. It shows similar decreasing trend as reported experimentally by the former researchers for these compounds [7]. However their dissimilar values of energy band gap may have been

**Table 3**
Some important phonon modes for $M_2YVO_6$; (M = Mg, Sr) perovskite oxides.

| Sr. No. | $Mg_2YVO_6$ | | | $Sr_2YVO_6$ | | |
|---|---|---|---|---|---|---|
| | Frequency ($cm^{-1}$) | IR active modes | Raman active modes | Frequency ($cm^{-1}$) | IR active modes | Raman active modes |
| 1 | 43.41 | Yes | No | 55.33 | Yes | No |
| 2 | 128.80 | Yes | No | 142.68 | Yes | No |
| 3 | 195.00 | Yes | No | 165.48 | Yes | No |
| 4 | 245.96 | – | Yes | 195.29 | Yes | No |
| 5 | 272.99 | No | Yes | 247.17 | Yes | No |
| 6 | 282.39 | Yes | No | 287.05 | Yes | No |
| 7 | 292.73 | No | Yes | 373.57 | Yes | No |
| 8 | 335.34 | Yes | No | 436.56 | Yes | No |
| 9 | 408.65 | Yes | No | 472.84 | Yes | No |
| 10 | 437.04 | No | Yes | 554.03 | Yes | No |
| 11 | 451.91 | Yes | No | 685.83 | Yes | No |
| 12 | 489.45 | Yes | No | 706.00 | Yes | No |
| 13 | 495.21 | No | Yes | 726.93 | Yes | No |
| 14 | 526.88 | Yes | No | 731.90 | No | Yes |
| 15 | 540.16 | No | Yes | 739.77 | No | Yes |
| 16 | 564.55 | Yes | No | 868.24 | No | Yes |
| 17 | 666.30 | No | Yes | 950.80 | No | Yes |
| 18 | 728.28 | No | Yes | 965.29 | No | Yes |

noticed owing to different space group ($P_2/m$) as reported in former studies, but we have opted ($P2_1/n$) for our calculations. It divulges that in our latter case ($Sr_2YVO_6$), the energy states in the conduction band have been happened comparatively close to the Fermi level, which may require less amount of energy to encroach these states. In fact, transition distance for valence electrons is reduced on increasing the ionic radius of A-site cations of our compounds. Moreover, $Sr_2YVO_6$ may holds comparatively small energy band gap owing to the similar decreasing tendency of the bond strength between Sr–O as compared to Mg–O [29].

The accumulative behavior of the energy states of the studied compounds within the energy interval −8 eV–15 eV, while using LDA + U approach, is displayed in Fig. 6(a) and 7(a), whereas Figs. 6(b) & 7(b) represents contribution at elemental level to foresee the element which is contributing more efficiently and effectively in conduction mechanism. One can also affirm formation/contribution of constituents by comparing their peaks appearing in (a) and (b) parts of each Figs. (6 and 7). The PDOS for $Mg_2YVO_6$ and $Sr_2YVO_6$ are shown in Fig. 6(c–f) & 7(c-f) respectively, which highlight contribution of the orbitals [30] of each constituent element of the considered compounds. It is noted from Fig. 6 (c) that Mg-*s* states have appeared around 6.20 eV energy along with its '*p*' states which are observed in higher energy span of the conduction band between 7.5 eV and 11.5 eV. Besides, few *s/p* states of magnesium atoms are found in valence band. As regard pseudo-states *'d'* of the yttrium elements (Fig. 6(d)) are found to be contributing more effectively in conduction band with its 1st prominent peak/highest state appeared at 8.80 eV followed by various other large range of the energy states between 9.60 eV and 12 eV. Although minimal contribution of 'Y' can also be seen in lower energy range/valence band. The large number of pseudo-states *'d-orbital'* of the vanadium elements (Fig. 6(e)) are found to be present around 2.20 eV in the conduction region near the Fermi level, which have been disappeared in between 2.57 and 4.80 eV. However, around 5.40 eV these states are reappeared with less density. In line with formerly reported quite obvious facts regarding anions of different perovskite oxides [27,31–34], O-*p* states in the considered compounds are found to be contributed in rein of the valence band adjacent to the Fermi level as displayed in Fig. 6(f).

As depicted in Fig. 7(c), localized *p* states of Sr are appeared near $F_E$ in the valence band between −0.40 and −1.96 eV energy with its subsequent occurrence around 12.60 eV in far region of the conduction band having divergent number of states. However, *s* states of Sr are embedded away from $F_E$ in the conduction region with their negligible presence in the valence band. Its highest energy states are located at 8.89 eV energy. And that Y-*d* states (Fig. 7(d)) are found maximally around 6.13 eV with significant 2nd highest peak of *d*-states around 9.55 eV energy range in the conduction region. Whereas Fig. 7(e) unveils that the pseudo-states of vanadium are positioned in lower energy range (at ~ 1.15 eV) of conduction band where the ytterbium and strontium states are either absent or insignificant. The vanadium states are also noticed in higher energy (around ~ 2.42 eV). Also the presence of significant pseudo-states of vanadium in the valence band around −2.33 eV manifest importance of these compounds. As obvious from our former studies, major contribution of O-2*p* states (Fig. 7(f)) is reported in the valence band near the Fermi level. Thereby, availability of the localized energy states in the conduction regions for both these compounds fortify the view point that the valence electrons may jump to these states while enhancing conductivity of such devices (i.e., optoelectronic, solar cells) whichever are fabricated for producing eternal energy. In addition, it has been noticed from Figs. 6(a) & 7(a) that the valence as well as the conduction regions of $Sr_2YVO_6$ hold greater number of localized electronic energy states than its counterpart ($Mg_2YVO_6$). Thus $Sr_2YVO_6$, being more stable, may contribute more effectively in conduction mechanism.

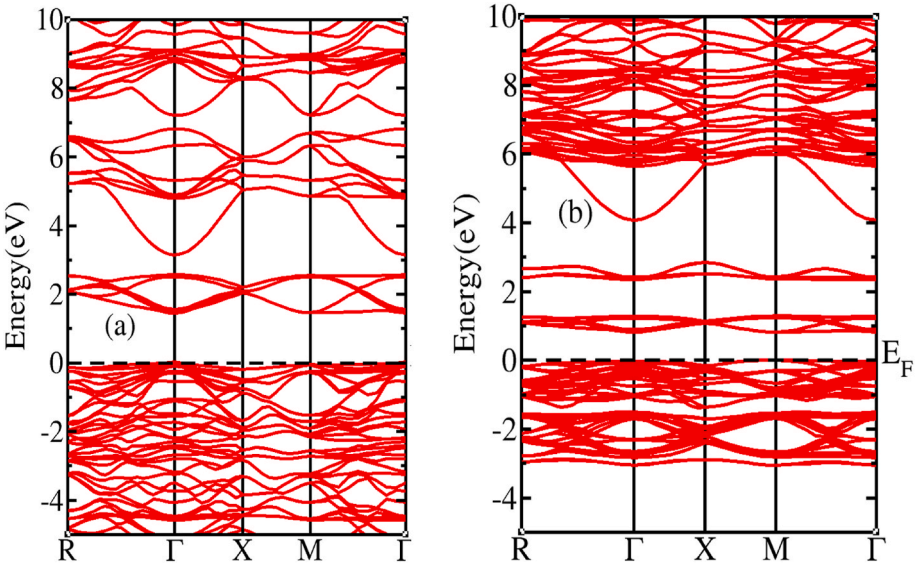


**Fig. 5.** The band structures plots for (a) $Mg_2YVO_6$ (b) $Sr_2YVO_6$ double perovskite oxides.

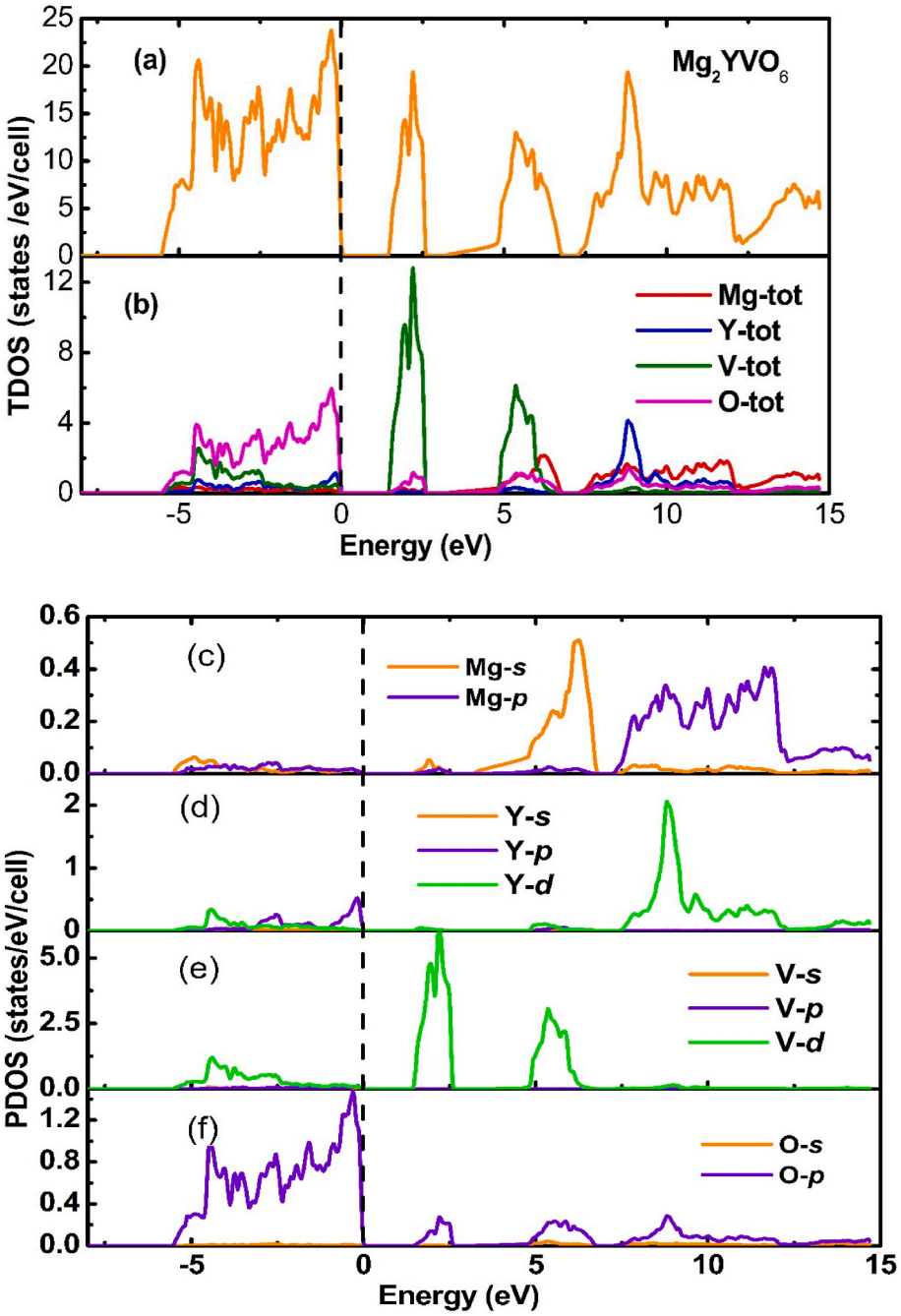


**Fig. 6.** (a–b) plots of total density of states (c–f) partial density of states of $Mg_2YVO_6$ double perovskite oxide.

### 3.4. Bond stiffness

Generally the deformation of any classical spring may be associated directly to the load/deforming force as obvious from the Hooke's law [35]. It is anticidated that cognate relation may subsists for chemical bonding, where bond strength can be determined by computing the bond stiffness. Also one can envisioned a fascinate shrinkage in lattice parameters on increasing the pressure systematically. The calculation of interatomic distance/bond length 'd' between various constituent atoms of any compound as a function of pressure is found to be an intriguing and appropriate panacea for assessing the bond stiffness. A significant reduction in interatomic distances as a function of pressure can be found in former report as well [36]. The ratio of bond stiffness (k) of the weakest bond to the strongest one may also be adjudicated for hunting whether or not the material is stiffer prior to its commercialization. To this intent, relative/normalized bond length ($\frac{d}{d_0}$) has been calculated as function of the pressure where $d_0$ represents the bond length at zero pressure. It is then gone-through second order polynomial fit ($Y = C_0 + C_1x + C_2x^2$), generally whose slope delineates the 1/k (where k is bond stiffness).

$$\frac{d}{d_0} = C_0 + C_1P + C_2P^2 \tag{3}$$

$$k = \left| \frac{d\left(d/d_0\right)}{dP} \right|^{-1} = |C_1 + 2C_2P|^{-1} \tag{4}$$

where $C_0$, $C_1$ and $C_2$ are coefficients of the polynomial fit. The total bond

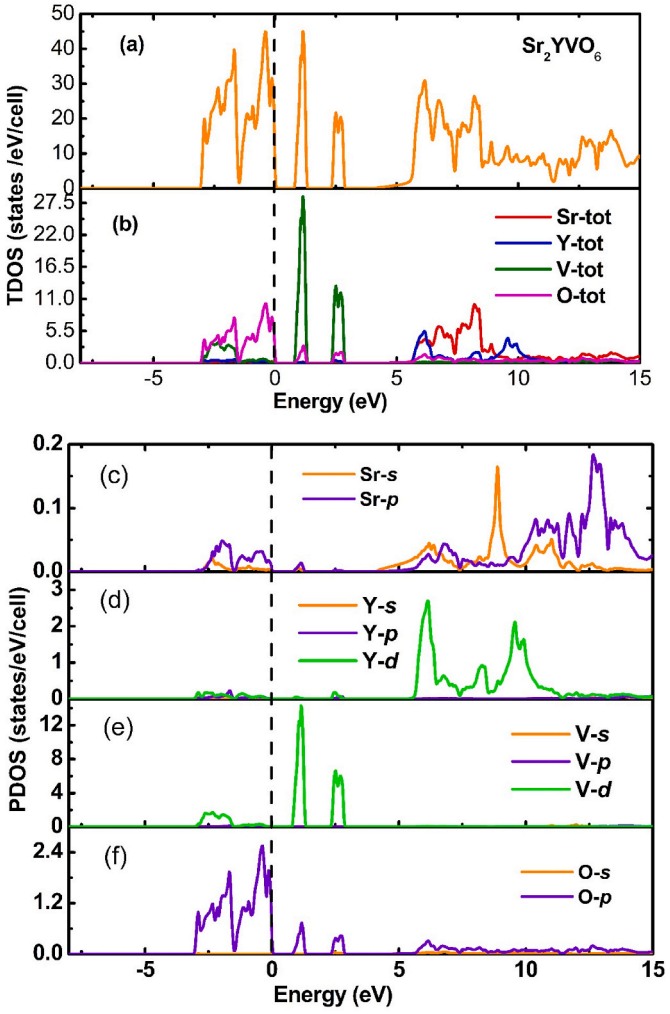


**Fig. 7.** (a–b) plots of total density of states (c–e) partial density of states of $Sr_2YVO_6$ double perovskite oxide.

stiffness of the compound may be calculated by the general expression such as $k_{total} = \sum_{i=1}^{n} k_i$ [32]. Table 4 portrays the bond length (Å) determined amid different constituent atoms of the $M_2YVO_6$; (M = Mg, Sr) at various pressure from 0 to 60 GPa with the group of 10 GPa. In consistent with our general acuity regarding the effect of pressure, the bond length is noted to be decreased on increasing pressure systematically from 0 GPa → 60 GPa. The bond length between $V^{5+}$ & $O^{2-}$ atoms like O2–V2, O8–V2, O11–V1, O5–V1 of $Mg_2YVO_6$ dwindled by 5.24% on escalation of the pressure merely from 0 GPa (1.92193 Å) to 10 GPa (1.82131 Å), followed by further 1.56% demesne on growing pressure from 10 GPa (1.82131 Å) to 20 GPa (1.79292 Å) and so on. Similar consistency in reduction of the bond lengths among different atoms has also been forecasted for $Sr_2YVO_6$. It is evident from the results summarized in Table 4 that the bond length may strongly be associated to ionic radii of A-cited divalent large cations ($Mg^{2+}$/$Sr^{2+}$) since comparative magnitudes of the bond length between different $Sr^{2+}$ and $O^{2-}$ atoms (O10–Sr2 = 2.56925 Å, O2–Sr4 = 2.57230) is found greater than their counter parts (O2–Mg4 = 2.20325, O12–Mg3 = 2.24894) at 0 GPa due to occurrence of the similar anomaly in their ionic radii ($Sr^{2+}$ > $Mg^{2+}$), and similar amenable trend can be observed at higher pressure as

**Table 5**
Coefficients ($C_0$, $C_1$, $C_2$) of second order polynomial fit of relative bond length ($d/d_0$) as a function of pressure P (GPa) and bond stiffness (k) for $M_2YVO_6$; (M = Mg, Sr) double perovskite oxides.

| Compounds | Bonds | $C_0$ | $C_1 \times 10^{-3}$ | $C_2 \times 10^{-5}$ | k (GPa) | Relative stiffness |
|---|---|---|---|---|---|---|
| $Mg_2YVO_6$ | O8–Mg2 | 0.9863 | −5.20 | 5.43 | 192 | 0.32 |
| | O12–Mg3 | 0.9890 | −5.18 | 5.15 | 193 | 0.32 |
| | O11–Y2 | 0.9859 | −3.82 | 4.03 | 262 | 0.43 |
| | O3–V1 | 0.9940 | −3.65 | 3.66 | 274 | 0.45 |
| | O5–O10 | 1.0000 | −1.64 | 0.38 | 610 | 1.00 |
| | O6–O7 | 0.9945 | −2.74 | 2.18 | 365 | 0.60 |
| $Sr_2YVO_6$ | O8–Sr2 | 0.9977 | −3.24 | 2.09 | 354 | 0.52 |
| | O12–Sr4 | 0.9955 | −3.21 | 2.07 | 358 | 0.53 |
| | O11–Y2 | 0.9986 | −1.98 | 1.38 | 587 | 0.88 |
| | O3–V1 | 0.9991 | −1.71 | 1.09 | 670 | 1.00 |
| | O5–O10 | 0.9999 | −1.61 | 0.41 | 654 | 0.98 |
| | O6–O7 | 0.9994 | −1.71 | 0.85 | 649 | 0.97 |

**Table 4**
Summary of the various bond lengths as a function of pressure ranging from 0 GPa to 60 GPa for $M_2YVO_6$; (M = Mg, Sr) double perovskite oxides.

| Bonds | | | | Bond length (Å) | | | | | | |
|---|---|---|---|---|---|---|---|---|---|---|
| | | | | 0 GPa | 10 GPa | 20 GPa | 30 GPa | 40 GPa | 50 GPa | 60 GPa |
| $Mg_2YVO_6$ | | | | | | | | | | |
| O2–V2 | O8–V2 | O11–V1 | O5–V1 | 1.92193 | 1.82131 | 1.79292 | 1.79000 | 1.78019 | 1.76936 | 1.74665 |
| O9–V1 | O6–V2 | O3–V1 | O12–V2 | 2.06659 | 1.97078 | 1.92293 | 1.90539 | 1.88172 | 1.87578 | 1.86750 |
| O4–Mg4 | O7–Mg1 | O1–Mg3 | O10–Mg2 | 2.10297 | 2.06194 | 2.06000 | 1.97467 | 1.95032 | 1.92633 | 1.92376 |
| O5–Mg3 | O8–Mg2 | O11–Mg1 | O2–Mg4 | 2.20325 | 2.02936 | 1.97538 | 1.94852 | 1.92370 | 1.91585 | 1.89585 |
| O6–Mg1 | O9–Mg4 | O3–Mg2 | O12–Mg3 | 2.24894 | 2.08440 | 2.02659 | 1.98923 | 1.95798 | 1.94287 | 1.92748 |
| O11–Y2 | O8–Y1 | O2–Y1 | O5–Y2 | 2.45428 | 2.29308 | 2.24346 | 2.23522 | 2.22449 | 2.21669 | 2.18880 |
| O1–Y1 | O10–Y2 | O7–Y1 | O4–Y2 | 2.58199 | 2.38351 | 2.38028 | 2.35000 | 2.32567 | 2.28092 | 2.26703 |
| O4–O11 | O2–O7 | O1–O8 | O5–O10 | 2.75523 | 2.70699 | 2.69972 | 2.62038 | 2.59678 | 2.54099 | 2.53635 |
| O1–O6 | O3–O4 | O9–O10 | O7–O12 | 2.68385 | 2.65730 | 2.63921 | 2.58943 | 2.56155 | 2.56096 | 2.53397 |
| O6–O7 | O3–O10 | O1–O12 | O4–O9 | 2.93415 | 2.81433 | 2.79036 | 2.73363 | 2.71073 | 2.67675 | 2.66099 |
| **$Sr_2YVO_6$** | | | | | | | | | | |
| O2–V2 | O8–V2 | O11–V1 | O5–V1 | 1.91191 | 1.88092 | 1.86242 | 1.84069 | 1.82222 | 1.80642 | 1.79589 |
| O9–V1 | O6–V2 | O3–V1 | O12–V2 | 1.91830 | 1.88555 | 1.85598 | 1.83655 | 1.82263 | 1.80754 | 1.79330 |
| O11–Y2 | O8–Y1 | O2–Y1 | O5–Y2 | 2.38826 | 2.33733 | 2.30055 | 2.27214 | 2.25281 | 2.23369 | 2.21685 |
| O1–Y1 | O10–Y2 | O7–Y1 | O4–Y2 | 2.40895 | 2.36114 | 2.32783 | 2.30045 | 2.27966 | 2.25903 | 2.24718 |
| O4–Sr4 | O7–Sr1 | O1–Sr3 | O10–Sr2 | 2.56925 | 2.49322 | 2.43148 | 2.38274 | 2.34204 | 2.30318 | 2.27352 |
| O5–Sr3 | O8–Sr2 | O11–Sr1 | O2–Sr4 | 2.57230 | 2.48022 | 2.41705 | 2.36864 | 2.32166 | 2.28634 | 2.25622 |
| O6–Sr1 | O9–Sr4 | O3–Sr2 | O12–Sr3 | 2.61517 | 2.55071 | 2.48454 | 2.43705 | 2.39472 | 2.36940 | 2.32815 |
| O6–O7 | O3–O10 | O1–O12 | O4–O9 | 2.74810 | 2.69857 | 2.66111 | 2.62974 | 2.59610 | 2.56608 | 2.54921 |
| O1–O6 | O3–O4 | O9–O10 | O7–O12 | 2.72620 | 2.67802 | 2.64185 | 2.61334 | 2.59424 | 2.57701 | 2.55741 |
| O4–O11 | O2–O7 | O1–O8 | O5–O10 | 2.74371 | 2.69633 | 2.66293 | 2.62747 | 2.57904 | 2.54438 | 2.52222 |

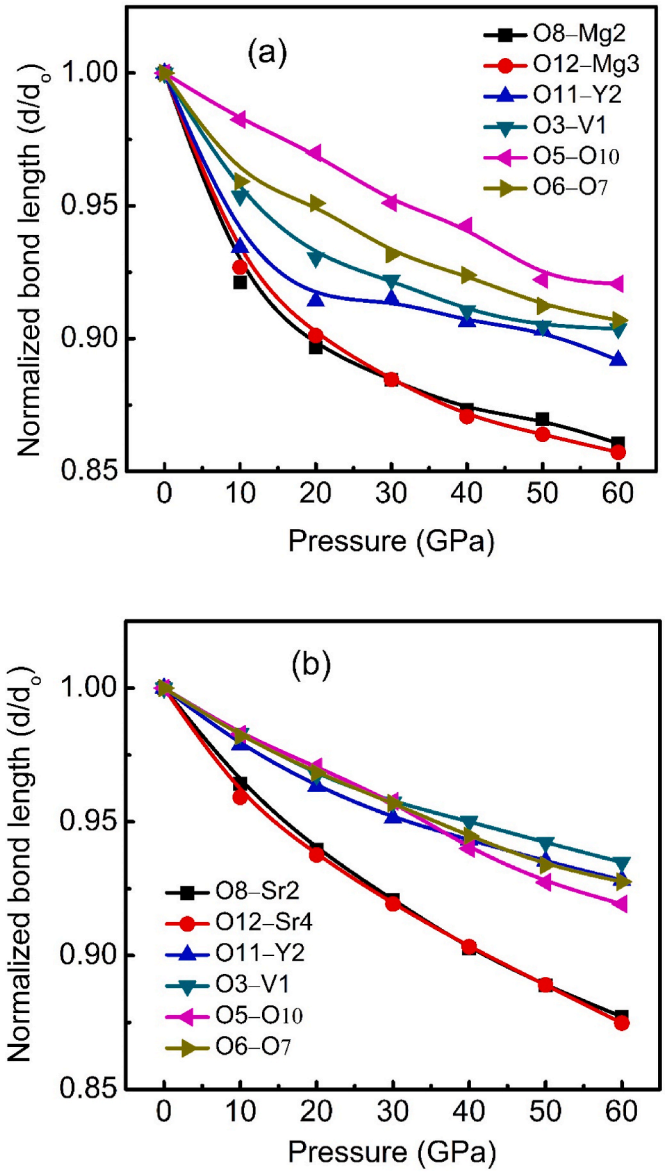


**Fig. 8.** Normalized bond length ($d/d_0$) as a function of external pressure from 0 to 60 GPa for (a) $Mg_2YVO_6$ (b) $Sr_2YVO_6$.

well. It basically indicates that $Mg^{2+}$ & $O^{-2}$ carry stronger bonds than $Sr^{2+}$ & $O^{2-}$. This clue dully reinforces our results pertaining to bulk modulus as summarized in Table 2, where $Mg_2YVO_6$ is claimed to be harder than its counterpart. To get further insights as claimed in the preceding work [37], our results pertaining to the energy band gap and bond length (summarized in Table 2 and 5) agree excellently with the fundamental understanding that the material of higher band gap may have short interatomic distances.

Table 5 illustrates coefficients of the second order polynomial fit of the relative bond lengths ($d/d_0$) as a function of pressure, and bond stiffness for $M_2YVO_6$; (M = Mg, Sr). Each $C_1$ holds negative value while $C_2$ is positive which may be attributed to some deep abstraction that deformation resistance, in both our compounds, upsurges with pressure. Comparatively, the value of relative bond stiffness for $Sr_2YVO_6$ is found greater than ½, whereas it is less than ½ for $Mg_2YVO_6$, which demonstrates that latter one could be an appropriate material for optoelectronic applications and that $Sr_2YVO_6$ seems equally useful for ceramic applications. Interestingly, the relative bond stiffness for similar atoms (O–O) in either case is found greater than ½. As shown in Fig. 8(a and b) the deepest slope (the red and black lines) is in consistent with the results tabulated in Table 4 that Mg/Sr–O bonds are longer (weaker) than the respective bonds appeared between Y/V and O atoms (stronger). Fig. 8(a and b) display the behavior of $d/d_0$ as function of pressure, where it can be noted for both our compounds that bond strength upsurges rapidly on increasing pressure, whereas an effective diminution in bond length has been noticed rigorously.

### 3.5. Optical properties

This class of characteristics of the studied materials describe how the sun-light interacts with the materials whenever falling on their surfaces. Here we discuss various optical parameters like complex dielectric function, absorptive behavior of the material, energy losses, complex refractive indices, optical trends and finally reflectivity of the light through the materials has been discussed.

#### 3.5.1. Dielectric function

The dielectric function comprises the two parts, one recognized as real part to specify degree of polarization and the second one measures the energy losses/absorption which is known as imaginary part [38]. As illustrated in Fig. 9(a), comparatively the static value (6.71) pertaining to real dielectric function $\varepsilon_1(0)$ for $Mg_2YVO_6$ is noted to be slighter than the related value (9.00) for $Sr_2YVO_6$, therefore later compound is appeared to be more apposite if used for manufacturing high-value aided capacitors. Additionally, the values of real dielectric function for $Mg_2YVO_6$ remains positive up to 10.0 eV photonic energy, however, thereafter it penetrate into the negative expanse where it reveals its metallic like character. So far as the value of $\varepsilon_1(\omega)$ for $Sr_2YVO_6$, it encroached into negative region initially for very short span in lower energy (from 1.61 eV to 1.92 eV) articulating its metallic behavior, which, however, reinstate behaviorally to positive region in higher

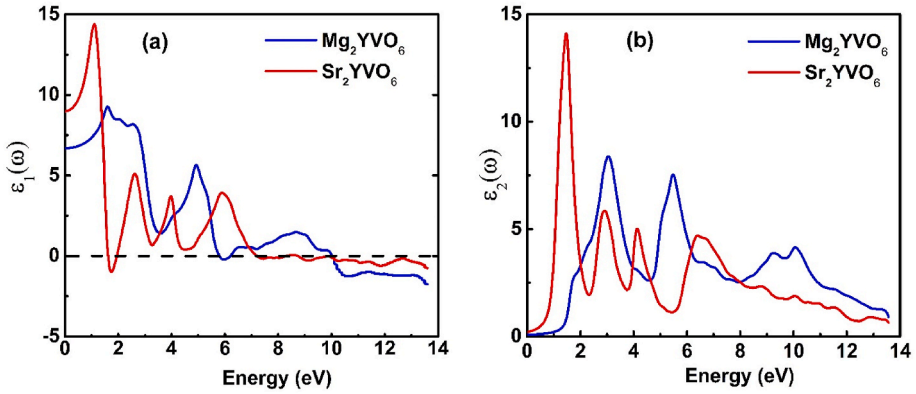


**Fig. 9.** The plots of (a) real and (b) imaginary dielectric constants drawn for $M_2YVO_6$; (M = Mg, Sr) double perovskite oxides.

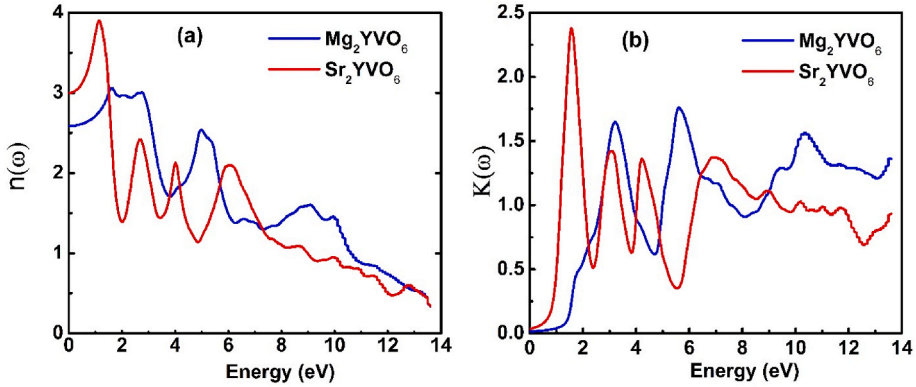


**Fig. 10.** The plots of (a) real refractive index and (b) imaginary refractive index (extinction coefficient) drawn for $M_2YVO_6$; (M = Mg, Sr) double perovskite oxides.

energy till 7.15 eV. Far flung to this energy edge it adopts similar leaning fashion toward negative energy rein as observed for $Mg_2YVO_6$.

The values of imaginary dielectric function $\varepsilon_2(\omega)$ for both these compounds are observed to be null till the energy approaches to their corresponding band gaps, because no transition takes place during this energy spell. Subsequently in higher energy, the values associated to $\varepsilon_2(\omega)$ grow strongly where 1st highest peak (8.42) for $Mg_2YVO_6$ appeared at 3.05 eV, while for $Sr_2YVO_6$ it has been noted as 14.21 at 1.47 eV energy. After appearing 1st peak, plethora of the fluctuations are observed till 13.60 eV energy, which might be associated to variations in inner band transitions. Particularly, decrement in values of $\varepsilon_2(\omega)$ beyond 10.0 eV energy endorse our viewpoint narrated about $\varepsilon_1(\omega)$ (Fig. 9(a)) that these compounds may have metallic like behavior in this peculiar expanse since they portray insufficient absorption of electromagnetic radiations in this energy spell.

### 3.5.2. *Refractive index and extinction coefficient*

The dimensionless and frequency dependent index of refraction ($n(\omega) = c/v$), where c is the speed of light in vacuum and v is its phase velocity, could be an effective remedy to determine the speed of light passing through the material [38,39]. The static value $n(0)$ (2.60) noted for $Mg_2YVO_6$ is smaller than the value (3.0) for $Sr_2YVO_6$ (Fig. 10(a)). In fact, greater magnitude of the refractive index lessen the angle of refraction, which further endorses our viewpoint that $Sr_2YVO_6$ is more absorbent material. Additionally, rather to depict unique behavior, the values of $n(\omega)$ exhibit trend similar to $\varepsilon_1(\omega)$ (Fig. 9(a)) which initially increase to some extent (3.07 for $Mg_2YVO_6$ and 3.91 for $Sr_2YVO_6$), while following the plethora of the fluctuations in higher energy range a robust reduction in refractive indices of both compounds has been noticed.

Whereas the imaginary component of the refractive index (usually recognized as an extinction coefficient $k(\omega)$) is most closely related to what extent the light absorbs in surface of the material, quite similar to the distinctive attributes as reflected by the imaginary dielectric function (Fig. 9(b)). As shown in Fig. 10(b), $k(\omega)$ remains zero till the threshold frequency is attained by the incident photons to knockout the energetic free electrons from the material's surface. In consistent with the above results obtained for $\varepsilon_2(\omega)$, highest value (1.77) of $k(\omega)$ noted for $Mg_2YVO_6$ at 5.62 eV is found to be shorter in magnitude as compared to its corresponding value (2.38) at 1.59 eV photonic energy for $Sr_2YVO_6$. Fig. 10(b) also ratifies ample absorption of light rays in lower energy range as well.

### 3.5.3. *Absorption coefficient and energy loss function*

Fig. 11(a) depicts the behavior between frequency dependent absorption coefficient α(ω) and photon energy ranging from 0 to 14 eV, which reflects no absorption initially owing to low frequency and lethargic photons falling on surfaces of the studied compounds. In nutshell, for semiconductors, α(ω) should be zero at the light frequency equal to the band gap. Therefore absorption of incident rays for our both compounds has merely been noticed as and when photons get energy equal to their work function. On increase of photonic energy beyond the limit of band gap, values of the α(ω) for these compounds upsurge drastically. However, certain fluctuations have been observed due to different rate of inner-band transitions. Providentially, incredible amount of α(ω) has been noticed at 13.60 eV energy for both compounds, i.e., $1.88 \times 10^6 cm^{-1}$ for $Mg_2YVO_6$ and $1.29 \times 10^6 cm^{-1}$ for $Sr_2YVO_6$. Apparently, the both compounds seem absorptive and appropriate candidate to be used for optoelectronic applications.

The loss function $L(\omega)$ versus photons energy graph is represented in Fig. 11(b), where $L(\omega)$ exhibits increasing trend on growing photonic energy to higher level. Nonetheless, the highest value of the loss function for both cases is very small, which apparently seems very small (i.e., 1.25) as compared to the absorption of light rays ($1.88 \times 10^6 cm^{-1}$ for

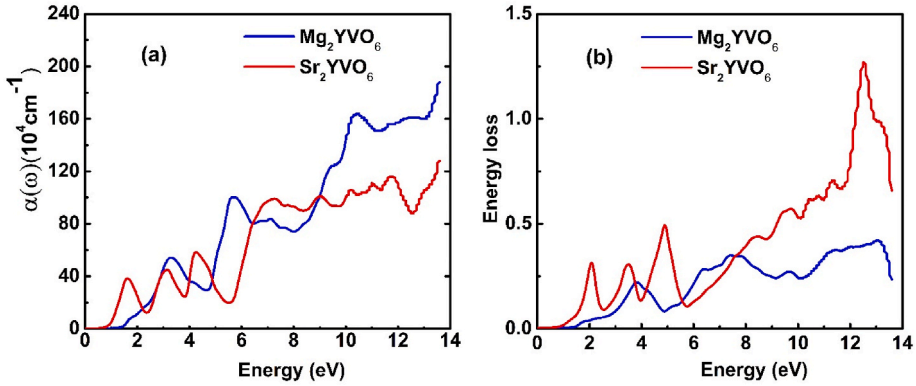


**Fig. 11.** The plots of (a) absorption constant and (b) loss function for $M_2YVO_6$; (M = Mg, Sr) double perovskite oxides.

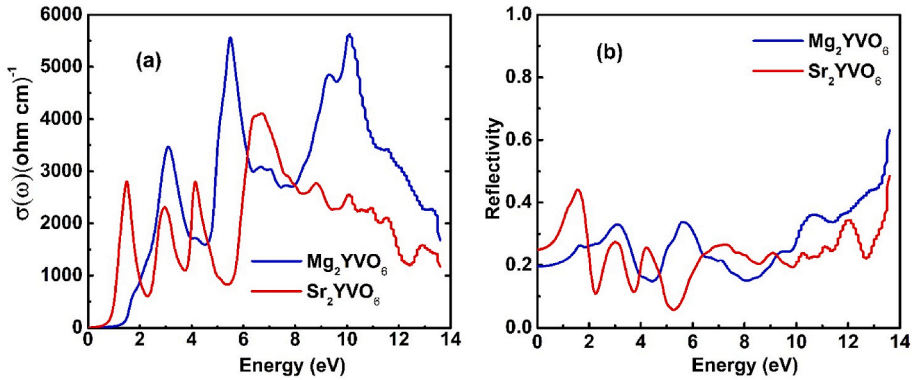


**Fig. 12.** The plots of (a) optical conductivity and (b) reflectivity for $M_2YVO_6$; (M = Mg, Sr) double perovskite oxides.

$Mg_2YVO_6$ and $1.29 \times 10^6 cm^{-1}$ for $Sr_2YVO_6$) into the surface of these materials.

### 3.5.4. Optical conductivity and reflectivity

Optical response of any material can be envisaged by optical conductivity ($\sigma = \alpha nc/4\pi$), which also depends upon $'\alpha'$ due to its direct relationship with frequency dependent $\sigma$, here $n$ = refractive index, $c$ = speed of light. Absorption of incident light rays solely depends upon the optical conductivity, no matter how slow the absorption is it. In our cases, initially the conduction seems to be zero at the light frequency equal to the band gap (Fig. 12(a)). 1st optical peak $3.50 \times 10^3 (ohm\ cm)^{-1}$ appeared at 3.09 eV for $Mg_2YVO_6$ can be seen as $2.81 \times 10^3 (ohm\ cm)^{-1}$ at lower energy (1.48 eV) for $Sr_2YVO_6$. A reasonable agreement has been noticed among the trends followed by the optical response and imaginary dielectric function (Fig. 9(b)). 2nd maxima appeared at 5.51 eV and 2.93 eV for $Mg_2YVO_6$ and $Sr_2YVO_6$, respectively may attributes the hybridization of V-3*d* localized energy states with pseudo states of anions. Subsequently, the highest density of $\sigma$ such as $5.65 \times 10^3 (ohm\ cm)^{-1}$ for $Mg_2YVO_6$ reflects the response of Mg-4*p* states and $4.11 \times 10^3 (ohm\ cm)^{-1}$ for $Sr_2YVO_6$ is associated with the hybridization of Sr and Y pseudo-states at photonic energy 10.10 eV and 6.71 eV, respectively.

Reflectivity response of the incident radiations from surfaces of the considered perovskites shown in Fig. 12(b) unveils very small values such as ~0.20 ($Mg_2YVO_6$) and ~0.25 ($Sr_2YVO_6$) of the static reflectivity R(0), thereby endorsing our claim that major portion of the incident rays, if fall on the surface of the studied materials, could be absorbed rather to reflect. Prompt decline which has been observed around 5.24 eV for $Sr_2YVO_6$ is associated to plasma resonance. Moreover, the appearance of magnitude of the reflectivity less than unity is an utter evidence that absorption can be happened on large scale ~$10^6$ $cm^{-1}$. Henceforth, the series of double perovskite oxides, i.e., $M_2YVO_6$; (M = Mg, Sr) may be reckoned an appropriate candidates to be employed for technological applications while devising optoelectronic appliances.

## 4. Concluding remarks

Here $M_2YVO_6$ (M = Mg, Sr) double perovskites oxides are simulated/modeled by using DFT based WIEN2K package in order to perform structural, optoelectronic and phonon calculations, wherein FPLAPW method has been opted for accurate calculation. The band structures of these compounds show that $Mg_2YVO_6$ have direct energy gap of 1.45 eV, whereas it has been noticed as 0.82 eV for $Sr_2YVO_6$. So these materials fall into the category of the semiconductors. The diminution of energy band gap for $Sr_2YVO_6$ may be attributed to the weak bond strength between Sr–O as compared to Mg–O. The various electronic states originated in conduction region at certain energy levels have revealed an effective contribution of the pseudo-states *'d'* of the yttrium elements, V-*d* and Mg/Sr-*p* states of $Mg_2YVO_6$ and $Sr_2YVO_6$. The value of relative bond stiffness for $Sr_2YVO_6$ is found greater than ½, whereas it is less than ½ for $Mg_2YVO_6$. As far as phonon's analysis have shown few soft modes of frequency for $Mg_2YVO_6$ while no imaginary modes of vibrations are observed for $Sr_2YVO_6$. Insignificant amount of the reflectivity with bountiful optical conduction/absorption of the electromagnetic radiations as determined through the optical analyses have stimulated us to declare that these compounds plausibly be an appropriate candidates for optoelectronic applications, if these are synthesized experimentally by the future researchers.

## CRediT authorship contribution statement

**Muhammad Iqbal Hussain:** Writing – review & editing, Writing – original draft, Visualization, Software, Resources, Methodology, Investigation, Formal analysis, Data curation, Conceptualization. **R.M. Arif Khalil:** Writing – review & editing, Writing – original draft, Visualization, Validation, Supervision, Project administration, Formal analysis.

## Declaration of competing interest

The authors declare that they have no known competing financial interests or personal relationships that could have appeared to influence the work reported in this paper.

## Data availability

Data will be made available on request.

## Acknowledgement

Authors are thankful and acknowledge the services of Dr. Shabbir Ahmad, Incharge Department of English for proofreading the manuscript to edit and improve the English language.

## References

[1] G. King, P.M. Woodward, Cation ordering in perovskites, J. Mater. Chem. 20 (28) (2010) 5785–5796.
[2] M.L. López, M.L. Veiga, J. Rodríguez-Carvajal, F. Fernández, A. Jerez, C. Pico, The monoclinic perovskite $La_2LiSbO_6$: a rietveld refinement of neutron powder diffraction data, Mat. Res. Bull. 27 (5) (1992) 647–654.
[3] T. Maiti, M. Saxena, P. Roy, Double perovskite ($Sr_2B'B''O_6$) oxides for high-temperature thermoelectric power generation-A review, J. Mater. Res. 34 (2018) 107–125.
[4] O. Sahnoun, H.B. Benziane, M. Sahnoun, M. Driz, C. Daul, *Ab initio* study of structural, electronic and thermodynamic properties of tungstate double perovskites $Ba_2MWO_6$ (M = Mg, Ni, Zn), Comput. Mater. Sci. 77 (2013) 316–321.
[5] M.S. Sheikh, D. Ghosh, A. Dutta, S. Bhattacharyya, T.P. Sinha, Lead free double perovskite oxides $Ln_2NiMnO_6$ (Ln = La, Eu, Dy, Lu), a new promising material for photovoltaic application, Mater. Sci. Eng. B. 226 (2017) 10–17.
[6] C.H. Su, Y.S. Wang, C.L. Huang, Characterization and microwave dielectric properties of $Mg_2YVO_6$ ceramic, J. Alloys and Comp. 641 (2015) 93–98.

[7] Y.A. Alsabah, A.T. Elden, M.S. AlSalhi, A.A. Elbadawi, M.A. Siddig, Structural and optical properties of $A_2YVO_6$ (A=Mg, Sr) double perovskite oxides, Results Phys 15 (2019) 1–6.
[8] W.J. Yin, B. Weng, J. Ge, Q. Sun, Z. Li, Y. Yan, Oxide perovskites, double perovskites and derivatives for electrocatalysis, photocatalysis, and photovoltaics, Energy Environ. Sci. 12 (2) (2019) 442–462.
[9] J. Kangsabanik, A. Alam, *Ab Initio* discovery of stable double perovskite oxides $Na_2BIO_6$ (B = Bi, In) with Promising Optoelectronic Properties, J. Phys. Chem. Lett. 11 (13) (2020) 5148–5155.
[10] A. Hossain, P. Bandyopadhyay, S. Roy, An overview of double perovskites $A_2B'B''O_6$ with small ions at A site: synthesis, structure and magnetic properties, J. Alloys and Comp. 740 (2018) 414–427.
[11] M. Nabi, D.C. Gupta, Study of the magneto-electronic, optical, thermal and thermoelectric applications of double perovskites $Ba_2MTaO_6$ (M= Er, Tm), RSC Adv 9 (28) (2019) 15852–15867.
[12] S.A. Mir, D.C. Gupta, Scrutinizing the stability and exploring the dependence of thermoelectric properties on band structure of 3d-3d metal-based double perovskites $Ba_2FeNiO_6$ and – $Ba_2CoNiO_6$, Sci. Rep. 11 (2021) 1–13.
[13] J. Kangsabanik, A. Alam, *Ab-initio* discovery of stable double perovskite oxides $Na_2BIO_6$ (B=Bi, in) with promising optoelectronic properties, J. Phys. Chem. Lett. 11 (13) (2020) 5148–5155.
[14] G. Vaitheeswaran, V. Kanchana, M. Alouani, A. Delin, *Ab initio* calculated X-ray magnetic circular dichroism of $Sr_2CrReO_6$, EPL 84 (2008) p1–p4.
[15] G. Vaitheeswarana, V. Kanchana, Pseudo-half-metallicity in the double perovskite $Sr_2CrReO_6$ from density-functional calculations, Appl. Phys. Lett. 86 (2005) 1–3.
[16] P. Blaha, K. Schwarz, G.K.H. Madsen, D. Kvasnicka, J. Luitz, WIEN2K, An Augmented Plane Wave + Local Orbitals Program for Calculating Crystal Properties, Karlheinz Schwarz, Techn. Universïtat Wien, Austria, 2001.
[17] R.M.A. Khalil, F. Hussain, A.M. Rana, M. Imran, G. Murtaza, Comparative study of polytype 2H-$MoS_2$ and 3R-$MoS_2$ systems by employing DFT, Phys. E: Low-Dimens. Syst. Nanostructures. 106 (2019) 338–345.
[18] G. Murtaza, I. Ahmad, B. Amin, A. Afaq, M. Maqbool, J. Maqssod, I. Khan, M. Zahid, Investigation of structural and optoelectronic properties of $BaThO_3$, Opt. Mater. 33 (2011) 553–557.
[19] O. Stenzel, The Kramers-Kronig Relations, vol. 44, Springer Berlin Heidelberg, 2005, pp. 61–68.
[20] F. Cicciarella, Semiconductor Optics: Kramers-Kronig Relations, Springer Nature Switzerland, 2014, pp. 125–129.
[21] S. Baroni, S. de Gironcoli, A. dal Corso, P. Giannozzi, Phonons and related crystal properties from density-functional perturbation theory, Rev. Mod. Phys. 73 (2) (2001) 515–562.
[22] C.J. Howard, P.W. Barnes, B.J. Kennedy, P.M. Woodward, Structures of the ordered double perovskites $Sr_2YTaO_6$ and $Sr_2YNbO_6$, Acta. Crystallogr. B. Struct. Sci. 61 (2005) 258–262.
[23] O. Sahnoun, H.B. Benziane, M. Sahnoun, M. Driz, C. Daul, *Ab initio* study of structural, electronic and thermodynamic properties of tungstate double perovskites $Ba_2MWO_6$ (M = Mg, Ni, Zn), Comput. Mater. Sci. 77 (2013) 316–321.
[24] K. Leng, Q. Tang, Y. Wei, Li Yang, Y. Xie, Z. Wu, X. Zhu, Recent advances in Re-based double perovskites: synthesis, structural characterization, physical properties, advanced applications and theoretical studies, AIP Adv 10 (2020) 1–31.
[25] S.M. Borchani, W.C.-R. Koubaa, M. Megdiche, Structural, magnetic and electrical properties of a new double-perovskite $LaNaMnMoO_6$ material, R. Soc. Open Sci. 4 (11) (2017) 1–16.
[26] N.A. Benedek, C.J. Fennie, Why are there so few perovskite ferroelectrics? J. Phys. Chem. C 117 (26) (2013) 13339–13349.
[27] M.I. Hussain, R.M.A. Khalil, S. Boota, F. Hussain, M. Imran, G. Murtaza, A.M. Rana, M.A. Sattar, The structural, electronic and dynamical investigations of $NdMn_2O_5$ and $La_2CoMnO_6$ for optoelectronic applications: a first Principles study, Optik 204 (2020) 1–9.
[28] M. Baskurt, I. Eren, M. Yagmurcukardes, H. Sahin, Vanadium dopant- and strain-dependent magnetic properties of single-layer $VI_3$, Appl. Surf. Sci. 508 (2020) 1–11.
[29] H.W. Eng, P.W. Barnes, B.M. Auer, P.M. Woodward, Investigations of the electronic structure of $d^0$ transition metal oxides belonging to the perovskite family, J. Solid State Chem. 175 (2003) 94–109.
[30] B. Ghebouli, M.A. Ghebouli, H. Choutri, M. Fatmi, T. Chihi, L. Louail, A. Bouhemadou, S. Bin-Omran, R. Khenata, H. Khachai, An *ab-initio* study of the structural, elastic, electronic, optical properties and phonons of the double perovskite oxides $Sr_2AlXO_6$ (X=Ta, Nb, V), Mater. Sci. Semicond. Process. 42 (2016) 405–412.
[31] M.I. Hussain, R.M.A. Khalil, F. Hussain, M. Imran, A.M. Rana, S. Kim, Investigations of structural, electronic and optical properties of $TMGaO_3$ (TM = Sc, Ti, Ag) perovskite oxides for optoelectronic applications: a first principles study, Mater. Res. Express. 7 (2020) 1–11.
[32] M.I. Hussain, R.M.A. Khalil, F. Hussain, M. Imran, A.M. Rana, S. Kim, Investigations of structural, electronic and optical properties of $YInO_3$ (Y = Rb, Cs, Fr) perovskite oxides using mBJ approximation for optoelectronic applications: a first principles study, Mater. Sci. Semicond. Process. 113 (2020) 1–9.
[33] M.I. Hussain, R.M.A. Khalil, F. Hussain, A.M. Rana, G. Murtaza, M. Imran, Probing the structural, electronic, mechanical strength and optical properties of tantalum-based oxide perovskites $ATaO_3$ (A=Rb, Fr) for optoelectronic applications: first-principles investigations, Optik 219 (2020) 1–10.
[34] M.I. Hussain, R.M.A. Khalil, F. Hussain, A.M. Rana, *Ab-initio* prediction of the structural, electronic and optical behavior of novel combinations of ternary perovskite oxides ATiO3 (A = Rb, Cs, Fr) using the Hubbard 'U' correction for optoelectronic devices, J. Comput. Electron. 19 (4) (2020) 1380–1388.
[35] Y. Bai, X. He, R. Wang, C. Zhu, An ab initio study on compressibility of Al-containing MAX-phase carbides, Int. J. Appl. Phys. 114 (2013) 1–12.
[36] X. He, Y. Bai, C. Zhu, M.W. Barsoum, Polymorphism of newly discovered $Ti_4GaC_3$: a first-principles study, Acta Mater 59 (14) (2011) 5523–5533.
[37] M. Pazoki, T. Edvinsson, Metal replacement in perovskite solar cell materials: chemical bonding effects and optoelectronic properties, R. Soc. Chem. Sustain. Energy Fuels. 2 (2018) 1430–1445.
[38] R. Ullah, M.A. Ali, G. Murtaza, A. Khan, A. Mahmood, *Ab initio* study for the structural, electronic, magnetic, optical, and thermoelectric properties of $K_2OsX_6$ (X=Cl, Br) compounds, Int. J. Energy Res. 44 (11) (2020) 1–15.
[39] A. Lamichhane, N.M. Ravindra, Energy gap-refractive index relations in perovskites, Materials 13 (2020) 1–16.